ELSEVIER

Signal Processing 67 (1998) 173–187

SIGNAL PROCESSING

The DS/SSMA systems using trellis coding with asymmetric PSK signal constellation

Seong Ill Park[a,b], Kwang Soon Kim[a], Hyung-Myung Kim[a], Iickho Song[a,*]

[a] *Department of Electrical Engineering, Korea Advanced Institute of Science and Technology (KAIST), 373-1 Guseong Dong, Yuseong Gu, Daejeon 305-701, South Korea*

[b] *Daewoo Electronics Co., Ltd., P.O. Box 8003, Seoul, South Korea*

Received 6 May 1997; received in revised form 21 January 1998

Abstract

We analyze the performance of direct-sequence spread spectrum multiple access (DS/SSMA) systems, which use trellis coding with asymmetric phase shift keying (PSK) modulation. By designing the signal constellation to be asymmetric, we obtain a performance gain for the DS/SSMA system over the systems using the traditional symmetric signal constellation. Bit error probability analysis of the proposed system is carried out for some cases. Examples are given to show the performance gain due to the asymmetry of the signal constellation. © 1998 Elsevier Science B.V. All rights reserved.

Zusammenfassung

Wir untersuchen die Eigenschaften von DS/SSMA (*Direct Access Spread Spectrum Multiple Access*) Systemen, welche eine Trellis Kodierung mit asymmetrischer PSK Modulierung benutzten. Durch die asymmetrische Gestaltung der Signalkonstellation erhalten wir verbesserte Eigenschaften des DS/SSMA Systems verglichen mit Systemen, die die traditionelle, symmetrische Signalkonstellation benutzen. Für einige Systeme wird eine Analyse der Bit-Fehlerwahrscheinlichkeiten für das vorgeschlagene System durchgeführt. Beispiele, die die Verbesserung aufgrund der asymmetrischen Signalkonstallation belegen, werden angegeben. © 1998 Elsevier Science B.V. All rights reserved.

Résumé

Nous analysons dans cet article les performances des systèmes à spectre étendu multi-accès à séquence directe (DS/SSMA), qui utilisent un codage en treillis avec une modulation de type décalage de phase (PSK) asymétrique. Nous obtenons, en synthétisant une constellation asymétrique, un gain en performances pour le système DS/SSMA vis-à-vis des systèms utilisant la constellation symétrique traditionnelle. L'analyse de la probabilité d'erreur sur les bits pour le système proposé est faite dans certains cas. Nous donnons des exemples qui mettent en évidence les gains en performances dus à l'utilisation d'une constellation asymétrique. © 1998 Elsevier Science B.V. All rights reserved.

Keywords: Asymmetric trellis coded modulation (ATCM); Direct sequence spread spectrum multiple access

* Corresponding author. Tel.: + 82-42-869-3445; fax: + 82-42-869-3410; e-mail: isong@sejong.kaist.ac.kr.

PII S0165-1684(98)00035-8

1. Introduction

Spread-spectrum (SS) communication systems have been extensively investigated and considered for practical applications: typical examples of the applications of SS communication systems are those in military communication and in commercial mobile communication. There exist primarily two SS techniques. One is the direct sequence (DS) SS, which is fundamentally an amplitude modulation technique, and the other is the frequency hopping (FH) SS, which is a frequency modulation technique. An SS communication system differs markedly from the time division (TD) and frequency division (FD) multiple access (MA) communication systems in that each transmitted signal in the SS communication system uses the entire frequency band of the system and the entire time of the communication.

In the past, coding and modulation were treated as separate operations with regard to overall system design. In [8], it has been shown that optimally designed rate $n/(n+1)$ trellis codes mapped into the conventional 2^{n+1}-point signal sets can provide a significant coding gain without bandwidth expansion when compared to the uncoded conventional 2^n-point signal sets. Optimization of the signal set in the modulation was not, however, considered in [8]. The DS/SSMA systems using PSK signal constellations were investigated in [5,6]. In [6], the probability of bit error of the DS/SSMA system with binary PSK (BPSK) modulation is obtained. In a coded additive white Gaussian noise (AWGN) environment, the optimum signal sets were obtained in [3] for the trellis coded system with asymmetric MPSK modulation. The performance of the DS/SSMA system using trellis coded modulation (TCM) was obtained in [9] in the no-fading case.

When the DS/SSMA systems are used with TCM, we get some coding gains over the convuentional scheme not using TCM [9]: it was assumed in [9] that the signal constellation was orthogonal. When the asymmetric TCM (ATCM) is used, however, we may get more coding gain than when the conventional or symmetric TCM (STCM) is used in the DS/SSMA systems. In this paper, we will use 'conventional' or 'STCM' to denote the TCM scheme with a symmetric signal constellation, and 'ATCM' to denote the TCM with asymmetric signal constellations as in [1]. In addition, since fading is generally present in SS systems, it is necessary to consider the effects of fading in designing the overall SS systems. In this paper, we will consider *DS/SSMA systems using the ATCM scheme* under the *fading channel* assumption, and investigate the performance of the ATCM DS/SSMA systems.

2. System model

We use the familiar system model, e.g. [4], of K users transmitting asynchronously over an AWGN fading channel. The transmitted signal of the kth user for a binary DS/SSMA system with ATCM can be expressed as

$$s^k(t) = \mathrm{Re}\{\sqrt{2P}x^k(t)\,a^k(t)\exp(\mathrm{j}2\pi f_c t + \mathrm{j}\varphi^k)\}, \tag{1}$$

where $P = E_s/(2T)$ is the power of the transmitted signal (the equal power assumption is made for convenience in presenting numerical results), T is the symbol period, f_c is the carrier frequency, φ^k is a random phase, E_s is the energy of the transmitted signal, Re stands for the real part, $\mathrm{j} = \sqrt{-1}$, and $a^k(t)$ is the DS spreading (pseudo-noise) sequence waveform. The kth user's complex coded symbol signal $x^k(t)$ is given by

$$x^k(t) = \sum_{n=-\infty}^{\infty} x_n^k P_T(t - nT), \tag{2}$$

where $P_T(\cdot)$ is a rectangular pulse of duration T and x_n^k is the complex coded symbol of the kth user during the nth symbol period. For MPSK signal constellation, we have

$$x_n^k = \exp(\mathrm{j}\theta_n^k), \quad x_n^k \in \{\mu_0, \mu_1, \ldots, \mu_{M-1}\}, \tag{3}$$

where θ_n^k is the phase of the nth symbol selected from the signal constellation by the information sequence $\{b_n^k\}_{n=-\infty}^{\infty}$. The symmetric and asymmetric signal constellations for the TCM schemes are shown in Fig. 1. The DS spreading sequence waveform $a^k(t)$ of period T is defined by

$$a^k(t) = \sum_{m=1}^{N} a_m^k \psi(t - (m-1)T_c), \quad 0 \leqslant t < T, \tag{4}$$

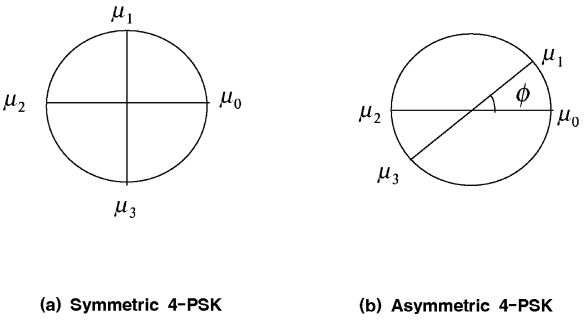

Fig. 1. The symmetric and asymmetric 4-PSK signal constellations for TCM schemes.

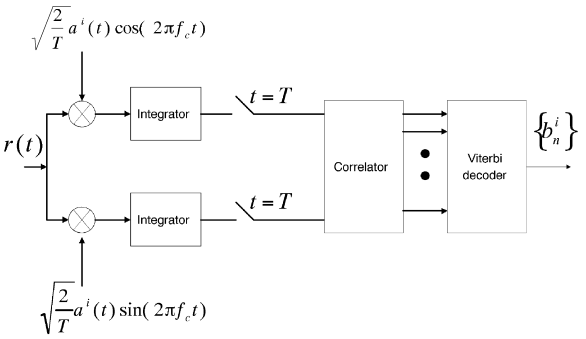

Fig. 2. The receiver structure.

where $a_m^k \in \{-1, +1\}$ is the mth chip of the spreading sequence of the kth user and $\psi(\cdot)$ is the chip waveform of duration T_c. It is usually assumed that $T = NT_c$ for some positive integer N.

Assuming an AWGN channel, the received signal can be expressed as

$$r(t) = \sum_{k=1}^{K} y^k(t - \tau^k) + \eta(t), \tag{5}$$

where τ^k is the time delay experienced by the signal received from user k and $\eta(t)$ is the AWGN with two-sided spectral density $N_0/2$. For a Rician fading channel, $y^k(t)$ is described by

$$y^k(t) = \mathrm{Re}\{\rho^k s^k(t)\exp(\mathrm{j}\varpi^k)\}, \tag{6}$$

where ρ^k is the Rician random variable representing the attenuation of the signal strength due to the fading, and ϖ^k is the phase shift uniformly distributed over $[0, 2\pi)$.

The receiver for each user is composed of two demodulation branches (the inphase (I) and quadrature (Q) branches), a correlator, and a Viterbi decoder. In each of the branches, $r(t)$ is multiplied by the despreading sequence for user i and a sine wave, and then integrated over $[0, T]$. This structure is shown in Fig. 2. After the demodulation through the I and Q demodulators, the sampled complex input y_n^i to the correlator can be expressed as

$$y_n^i = \rho_n^i x_n^i + z_n^i + \eta_n^i, \tag{7}$$

where z_n^i represents the inter-user interference by the $K-1$ users, and η_n^i is the noise term.

The interference z_n^i is represented by [6]

$$z_n^i = \frac{1}{T}\sum_{k=1,k\neq i}^{K}[x_{n-1}^k R_{k,i}(\tau^k) + x_n^k \hat{R}_{k,i}(\tau^k)],$$
$$0 \leqslant \tau^k < T, \tag{8}$$

where

$$\begin{aligned} R_{k,i}(\tau^k) &= \int_0^{\tau^k} a^k(t - \tau^k)a^i(t)\,\mathrm{d}t \\ &= C_{k,i}(l - N)\hat{R}_\psi(\tau^k - lT_c) \\ &\quad + C_{k,i}(l + 1 - N)R_\psi(\tau^k - lT_c) \end{aligned} \tag{9}$$

and

$$\begin{aligned} \hat{R}_{k,i}(\tau^k) &= \int_{\tau^k}^{T} a^k(t - \tau^k)a^i(t)\,\mathrm{d}t \\ &= C_{k,i}(l)\hat{R}_\psi(\tau^k - lT_c) \\ &\quad + C_{k,i}(l + 1)R_\psi(\tau^k - lT_c) \end{aligned} \tag{10}$$

are the even and odd continuous-time partial cross correlation functions, respectively. In Eqs. (9) and (10), the partial autocorrelation functions of the chip waveform are defined by

$$R_\psi(s) = \int_0^s \psi(t)\psi(t + T_c - s)\,\mathrm{d}t \tag{11}$$

and

$$\hat{R}_\psi(s) = \int_s^{T_c} \psi(t)\psi(t - s)\,\mathrm{d}t, \tag{12}$$

and the aperiodic cross-correlation function is defined by

$$C_{k,i}(l)=\begin{cases}\sum_{j=0}^{N-1-l}a_j^k a_{j+l}^i, & 0\leqslant l\leqslant N-1,\\ \sum_{j=0}^{N-1+l}a_{j-l}^k a_j^i, & 1-N\leqslant l<0,\\ 0 & |l|\geqslant N.\end{cases} \quad (13)$$

Based on the above formulation, we will investigate the performance of the DS/SSMA system using ATCM in the next section. We will first obtain the pairwise error probability and then the bit error probability bounds.

3. Performance analysis

3.1. Taylor expansion method

The performance of a trellis coded SSMA communication system can be evaluated using the transfer function bound technique which has been developed for evaluating the performance of convolutional codes and recently applied to evaluating the performance of trellis codes [1]. The generalized transfer function bound method involves calculating pairwise error probabilities using the Chernoff bound and summing over all possible error patterns using the union bound. Since every user can be assumed to have the same performance, without loss of generality, we will drop the user index k in x_n^k, y_n^k and z_n^k for notational convenience.

Consider the complex coded symbol sequence $\boldsymbol{x}=(\ldots,x_1,x_2,x_3,\ldots)$, complex demodulated sequence $\boldsymbol{y}=(\ldots,y_1,y_2,y_3,\ldots)$, and complex interuser interference sequence $\boldsymbol{z}=(\ldots,z_1,z_2,z_3,\ldots)$. The conditional pairwise error probability $P(\boldsymbol{x}\to\hat{\boldsymbol{x}}|\boldsymbol{w})$ of decoding $\boldsymbol{x}$ as $\hat{\boldsymbol{x}}$ is given by

$$P(\boldsymbol{x}\to\hat{\boldsymbol{x}}|\boldsymbol{w})=\Pr\{m(\boldsymbol{y},\hat{\boldsymbol{x}};\boldsymbol{w})\geqslant m(\boldsymbol{y},\boldsymbol{x};\boldsymbol{w})|\boldsymbol{x}\}, \quad (14)$$

where $m(\boldsymbol{y},\boldsymbol{x};\boldsymbol{w})$ is a metric and $\boldsymbol{w}=(\ldots,w_1,w_2,w_3,\ldots)$ is a side information sequence. Applying the Chernoff bound results in

$$P(\boldsymbol{x}\to\hat{\boldsymbol{x}}|\boldsymbol{w})\leqslant\prod_{n\in v}E\{\exp[\lambda\{m(y_n,\hat{x}_n;w_n)-m(y_n,x_n;w_n)\}]|\boldsymbol{x}\}, \quad (15)$$

where v is the set of all n such that $x_n\neq\hat{x}_n$ and λ is the Chernoff parameter. Using

$$m(y_n,x_n;w_n)=-|y_n-\rho_n x_n|^2 \quad (16)$$

as the metric [1] under the perfect side information assumption, we get

$$P(\boldsymbol{x}\to\hat{\boldsymbol{x}}|\boldsymbol{\rho})\leqslant\prod_{n\in v}E\{\exp[\lambda(|y_n-\rho_n x_n|^2-|y_n-\rho_n\hat{x}_n|^2)]\}, \quad (17)$$

from Eq. (15), where $\boldsymbol{\rho}=(\ldots,\rho_1,\rho_2,\rho_3,\ldots)$. Simplifying Eq. (17) gives

$$P(\boldsymbol{x}\to\hat{\boldsymbol{x}}|\boldsymbol{\rho})\leqslant\prod_{n\in v}\exp\{-\lambda\rho_n^2|x_n-\hat{x}_n|^2\}\times E\{\exp[-2\lambda\rho_n\,\mathrm{Re}\{\eta_n(x_n-\hat{x}_n)^*\}]\}\times E\{\exp[-2\lambda\rho_n\,\mathrm{Re}\{z_n(x_n-\hat{x}_n)^*\}]\}. \quad (18)$$

The first expectation of Eq. (18) can be obtained as [1]

$$E\{\exp[-2\lambda\rho_n\,\mathrm{Re}\{\eta_n(x_n-\hat{x}_n)^*\}]\}=\exp(2\lambda^2\rho_n^2\sigma_\eta^2|x_n-\hat{x}_n|^2), \quad (19)$$

and the second expectation of Eq. (18), from Taylor series expansion, is

$$E\{\exp[-2\lambda\rho_n\,\mathrm{Re}\{z_n(x_n-\hat{x}_n)^*\}]\}=E\left\{\sum_{m=0}^{\infty}\frac{1}{m!}[-2\lambda\rho_n\mathrm{Re}\{z_n(x_n-\hat{x}_n)^*\}]^m\right\}, \quad (20)$$

from which

$$P(\boldsymbol{x}\to\hat{\boldsymbol{x}}|\boldsymbol{\rho})\leqslant\prod_{n\in v}\exp\{-\lambda\rho_n^2|x_n-\hat{x}_n|^2(1-2\lambda\sigma_\eta^2)\}\times E\left\{\sum_{m=0}^{\infty}\frac{1}{m!}[-2\lambda\rho_n\,\mathrm{Re}\{z_n(x_n-\hat{x}_n)^*\}]^m\right\}. \quad (21)$$

Since the optimum value λ_o of λ which minimizes the right-hand side of Eq. (21) cannot be obtained in a closed form, we will obtain a suboptimum

value λ_s by approximating Eq. (20). Now

$$E\left\{\sum_{m=0}^{\infty}\frac{1}{m!}[-2\lambda\rho_n \mathrm{Re}\{z_n(x_n-\hat{x}_n)^*\}]^m\right\}$$
$$=\sum_{m=0}^{\infty}\frac{(-2\lambda\rho_n)^m}{m!}E\{[\mathrm{Re}\{z_n(x_n-\hat{x}_n)^*\}]^m\}$$
$$=1-2\lambda\rho_n E\{\mathrm{Re}\{z_n(x_n-\hat{x}_n)^*\}\}$$
$$+2\lambda^2\rho_n^2 E\{\mathrm{Re}^2\{z_n(x_n-\hat{x}_n)^*\}\}+\text{h.o.t}$$
$$\cong 1+2\lambda^2\rho_n^2 E\{\mathrm{Re}^2\{z_n(x_n-\hat{x}_n)^*\}\}. \quad (22)$$

This approximation is reasonable since the odd moments of $\mathrm{Re}\{z_n(x_n-\hat{x}_n)^*\}$ are zero when the density function of z_n is even [2]. In addition, it is shown in Appendix A that the approximation (22) is meaningful when the SNR is low: when the SNR is high, some of the higher-order terms should be included if we are to find a 'more correct' value of λ_s.

Then Eq. (21) can be written as

$$P(\boldsymbol{x}\to\hat{\boldsymbol{x}}|\boldsymbol{\rho})\leqslant\prod_{n\in v}\exp\{-\lambda\rho_n^2|x_n-\hat{x}_n|^2(1-2\lambda\sigma_\eta^2)\}$$
$$\times(1+\lambda^2\rho_n^2|x_n-\hat{x}_n|^2\sigma_z^2). \quad (23)$$

To obtain λ_s, let us differentiate any term on the right-hand side of Eq. (23) with respect to λ. It can be shown that

$$\lambda_s=-\frac{b}{3a}-\frac{2^{1/3}Q}{3a(R+\sqrt{4Q^3+R^2})^{1/3}}$$
$$+\frac{(R+\sqrt{4Q^3+R^2})^{1/3}}{3\cdot 2^{1/3}a}, \quad (24)$$

where

$$Q=48|x_n-\hat{x}_n|^6\rho_n^6\sigma_\eta^4\sigma_z^2-|x_n-\hat{x}_n|^8\rho_n^8\sigma_z^4$$
$$+24|x_n-\hat{x}_n|^6\rho_n^6\sigma_\eta^2\sigma_z^4,$$
$$R=288|x_n-\hat{x}_n|^{10}\rho_n^{10}\sigma_\eta^4\sigma_z^4+2|x_n-\hat{x}_n|^{12}\rho_n^{12}\sigma_z^6$$
$$-72|x_n-\hat{x}_n|^{10}\rho_n^{10}\sigma_\eta^2\sigma_z^6,$$
$$a=4|x_n-\hat{x}_n|^4\rho_n^4\sigma_\eta^2\sigma_z^2$$

and

$$b=-|x_n-\hat{x}_n|^4\rho_n^4\sigma_z^2.$$

It turns out that a direct use of Eq. (24) in Eq. (23) to obtain the upper bound of $P(\boldsymbol{x}\to\hat{\boldsymbol{x}}|\boldsymbol{\rho})$ by integrating the right-hand side of Eq. (23) with respect to ρ_n still results in an intractable expression. In order to alleviate the problem, let us approximate Eq. (24) as

$$\lambda_s\cong\frac{1}{4\sigma_\eta^2}. \quad (25)$$

Derivations of the results (24) and (25) are described in Appendix B. An implication of Eq. (25) is that, for an optimum ATCM system, the effects of multiuser interference may be ignored to some degree if the code length is large enough: if, in addition, the number of users is large, interferences can be modeled as Gaussian random signals [2] and we have only to consider the effects of Gaussian disturbances (noise and interference) and fading. In other words, under such circumstances, the effects of the additive noise and fading dominate over those of the multiuser interference. Note that if we let $\sigma_n^2\to\sigma_n^2+\sigma_z^2$, the value (25) becomes the value of λ when the interference is assumed to be Gaussian noise as we shall see in Section 3.2.

Using Eq. (25), Eq. (21) becomes

$$P(\boldsymbol{x}\to\hat{\boldsymbol{x}}|\boldsymbol{\rho})\leqslant\prod_{n\in v}\left\{\sum_{m=0}^{\infty}c_m\rho_n^{2m}\right\}\exp(-\zeta\rho_n^2), \quad (26)$$

where

$$\zeta=\frac{|x_n-\hat{x}_n|^2}{4}\frac{1}{2\sigma_n^2} \quad (27)$$

and

$$c_m=\left\{\frac{|x_n-\hat{x}_n|^2}{4}\frac{1}{4\sigma_\eta^4}\right\}^m\left\{\frac{1}{(2m)!}\right\}^2\frac{2}{(2m+1)}\frac{K-1}{N},$$
$$m=1,2,\ldots, \quad (28)$$

with $c_0=1$.

The parameter ρ_n can be modeled to be a Rician variable with a parameter L representing the ratio of the power in the direct component to that in the diffuse components. Note that a large value of L means a weak fading environment. The pdf of the

normalized (unit mean squared value) variable ρ_n is given by [1]

$$f(\rho) = 2\rho(1+L)\exp[-\{L+\rho^2(1+L)\}] \times I_0\{2\rho\sqrt{L(L+1)}\}, \quad (29)$$

where $I_0(\cdot)$ is the zeroth-order modified Bessel function of the first kind.

From Eqs. (26) and (29), the upper bound of the unconditional pairwise error probability is obtained to be

$$P(\boldsymbol{x}\to\hat{\boldsymbol{x}}) \leqslant \prod_{n\in v}\int_0^\infty \exp(-\zeta\rho_n^2)\left\{\sum_{m=0}^{\infty} c_m\rho_n^{2m}\right\} f(\rho_n)\,\mathrm{d}\rho_n = \prod_{n\in v}\sum_{m=0}^{\infty}\frac{m!(1+L)c_m}{(1+\zeta+L)^{m+1}} \times L_m^0\left[-\frac{L(1+L)}{1+\zeta+L}\right]\exp\left(\frac{-\zeta L}{1+\zeta+L}\right), \quad (30)$$

where

$$L_\varepsilon^\alpha(x) = \frac{1}{\varepsilon!}\mathrm{e}^x x^{-\alpha}\frac{\mathrm{d}^\varepsilon}{\mathrm{d}x^\varepsilon}(\mathrm{e}^{-x}x^{\varepsilon+\alpha}) \quad (31)$$

is the Laguerre polynomial.

Let us now obtain the bit error probability bound using the transfer function bound method. The bit error probability is known to be bounded as

$$P_\mathrm{b} \leqslant \frac{1}{2\gamma}\frac{\partial}{\partial I}T(D,I)|_{I=1}, \quad (32)$$

where T is the transfer function, D is the distance parameter, I is the parameter representing that a branch transition occurred by the input data bit 1, and γ is the number of information bits per coded symbol. Since the transfer function of the 1/2 rate and 1 state ATCM is [1]

$$T(D,I) = \frac{ID^{4(1+2\alpha)/(1+\alpha)}}{1-ID^{4(1+\alpha)}}, \quad (33)$$

where $\alpha = \tan^2\phi$, we have

$$P_\mathrm{b} \leqslant \sum_{i=1}^{\infty}\frac{i}{2}D^{4(i+2\alpha)/(1+\alpha)} = \sum_{i=1}^{\infty}\frac{i}{2}P(\boldsymbol{x}\to\hat{\boldsymbol{x}})|_{\text{event } i}, \quad (34)$$

with event $k, k = 1,2,\ldots$, defined as in Fig. 3. In Fig. 3, k represents the number of error branches, or the number of errors. In Fig. 3, we assumed that $\boldsymbol{x} = \boldsymbol{x}_0 = (\ldots,\mu_0,\mu_0,\mu_0,\ldots)$ without loss of generality.

From Eq. (30), we easily have

$$\begin{aligned} &P(\boldsymbol{x}\to\hat{\boldsymbol{x}}) \leqslant P_1 P_2,\\ &P(\boldsymbol{x}\to\hat{\boldsymbol{x}}) \leqslant P_1 P_2 P_3,\\ &P(\boldsymbol{x}\to\hat{\boldsymbol{x}}) \leqslant P_1 P_2 P_3^2,\\ &\vdots \end{aligned} \quad (35)$$

for events $1,2,3,\ldots$, respectively, where

$$P_i = \sum_{m=0}^{\infty}\frac{m!(1+L)\xi_{m,i}}{(1+\zeta_i+L)^{m+1}}L_m^0\left[-\frac{L(1+L)}{1+\zeta_i+L}\right] \times\exp\left(\frac{-\zeta_i L}{1+\zeta_i+L}\right), \quad i=1,2,3 \quad (36)$$

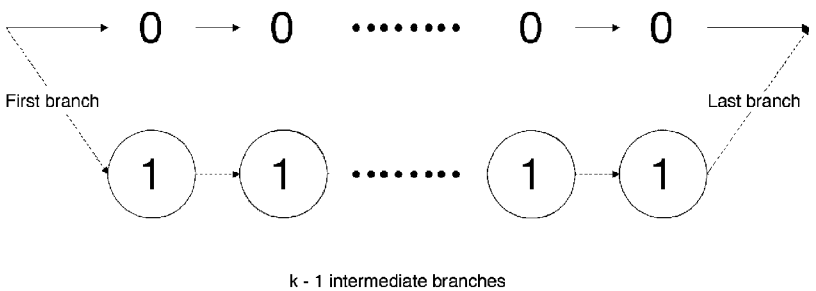

Fig. 3. Error event k: a dashed line is an error branch. k is a number of errors. If $k=1$, 1 intermediate branch occurs, that is, there is one error.

(in fact, P_i is the branch error probability of decoding μ_i when μ_0 was indeed sent with μ_i shown in Fig. 1). In Eq. (36)

$$\zeta_1 = \frac{1}{2\sigma_n^2}\sin^2\left(\frac{\phi}{2}\right),$$

$$\zeta_2 = \frac{1}{2\sigma_n^2},$$

$$\zeta_3 = \frac{1}{2\sigma_n^2}\cos^2\left(\frac{\phi}{2}\right),$$

$$\xi_{m,1} = \beta_m \sin^2\left(\frac{\phi}{2}\right),$$

$$\xi_{m,2} = \beta_m,$$

$$\xi_{m,3} = \beta_m \cos^2\left(\frac{\phi}{2}\right) \tag{37}$$

and

$$\beta_m = \left\{\frac{1}{2\sigma_\eta^4}\right\}^{2m}\left\{\frac{1}{(2m)!}\right\}^2 \frac{2}{(2m+1)}\frac{K-1}{N}. \tag{38}$$

In the expressions of ζ_i and $\xi_{m,i}, i = 1, 2, 3$, we used the facts that

$$|x_n - \hat{x}_n|^2 = 4\sin^2\left(\frac{\phi}{2}\right), \tag{39}$$

$$|x_n - \hat{x}_n|^2 = 4\cos^2\left(\frac{\phi}{2}\right) \tag{40}$$

and

$$|x_n - \hat{x}_n|^2 = 4 \tag{41}$$

for the first, last and intermediate branches, respectively. From Eqs. (34)–(36), we have

$$P_b \leqslant \frac{1}{2}(P_1P_2 + 2P_1P_2P_3 + 3P_1P_2P_3^2 + \cdots)$$

$$= \frac{1}{2}\sum_{i=0}^{\infty} iP_1P_2P_3^{i-1} = \frac{1}{2}\frac{P_1P_2}{(1-P_3)^2}. \tag{42}$$

We have so far obtained the pairwise error probability and bit error probability bounds of the DS/SSMA system with 1/2 rate ATCM scheme without assuming any specific distribution for the interuser interference.

3.2. Gaussian approximation

In Section 3.1, we did not assume that the interference is Gaussian. Let us now investigate if the Gaussian assumption would have any influence on the error probabilities. Assuming that the interference is Gaussian and that the in-phase and quadrature components of the interference are independent, we easily get

$$P(\boldsymbol{x} \to \hat{\boldsymbol{x}}|\boldsymbol{\rho}) \leqslant \prod_{n\in v}\exp\{-[\lambda\rho^2|x_n - \hat{x}_n|^2 \times \{1 - 2\lambda(\sigma_\eta^2 + \sigma_z^2)\}]\}, \tag{43}$$

as a direct application of the result in [2]. Since the Chernoff parameter λ_G optimizing Eq. (43) is

$$\lambda_G = \frac{1}{4(\sigma_\eta^2 + \sigma_z^2)}, \tag{44}$$

we have

$$P(\boldsymbol{x} \to \hat{\boldsymbol{x}}|\boldsymbol{\rho}) \leqslant \prod_{n\in v}\exp\left\{-\frac{\rho_n^2|x_n - \hat{x}_n|^2}{8(\sigma_\eta^2 + \sigma_z^2)}\right\} \tag{45}$$

and

$$P(\boldsymbol{x} \to \hat{\boldsymbol{x}}) = \prod_{n\in v}\int_0^\infty \exp\left\{-\frac{\rho_n^2|x_n - \hat{x}_n|^2}{8(\sigma_\eta^2 + \sigma_z^2)}\right\} f_{\rho_n}(\rho_n)\,\mathrm{d}\rho_n$$

$$= \prod_{n\in v}\frac{1+L}{1+\zeta+L}\exp\left\{-\frac{\zeta L}{1+\zeta+L}\right\}, \tag{46}$$

where

$$\zeta = \frac{|x_n - \hat{x}_n|^2}{4}\frac{1}{2(\sigma_\eta^2 + \sigma_z^2)}. \tag{47}$$

Thus, for the 1/2 rate ATCM scheme, the upper bound of the bit error probability is

$$P_b \leqslant \frac{1}{2}\frac{P_1P_2}{(1-P_3)^2}, \tag{48}$$

where

$$P_i = \frac{1+L}{1+\zeta_i+L}\exp\left(-\frac{\zeta_i L}{1+\zeta_i+L}\right),$$

$$i = 1, 2, 3, \tag{49}$$

$$\zeta_1 = \frac{1}{2(\sigma_\eta^2 + \sigma_z^2)} \sin^2\left(\frac{\phi}{2}\right), \tag{50}$$

$$\zeta_2 = \frac{1}{2(\sigma_\eta^2 + \sigma_z^2)} \tag{51}$$

and

$$\zeta_3 = \frac{1}{2(\sigma_\eta^2 + \sigma_z^2)} \cos^2\left(\frac{\phi}{2}\right). \tag{52}$$

As we can see in Eqs. (36) and (49), the two bit error probability bounds Eqs. (42) and (48) will be different in general. In Section 4, we will partly show the effects of the difference between Eqs. (36) and (49) on the upper bound of the bit error probability, via numerical analysis.

4. Numerical results

In this section, let us consider some numerical analysis based on the results in Section 3. The performance of the ATCM DS/SSMA scheme will naturally vary for different values of the rotation angle ϕ. If the rotation angle is $\pi/2$, then the ATCM has the same performance as the STCM: for the Gaussian approximation case, we can clearly see this using Eqs. (48)–(52), when $\phi = \pi/2$, which is equivalent to the results of [1]. Let us define the optimum (rotation) angle as the rotation angle which minimizes the bit error probability bound (42). The optimum angle is obviously a function of the system parameters, K, L, N and SNR. Since the optimum angle cannot be obtained in a closed form, we use numerical analysis to obtain the optimum angle.

In Fig. 4, the bit error probability versus the rotation angle is plotted for several values of K and N, when $L = 10$ and SNR $= 10$ dB. As we can see in this figure, the bit error probability has a minimum: the optimum angle becomes larger as the code length N becomes longer. The effects of the number K of users on the optimum angle and on the bit error probability are larger for short code length N than for long code length. In addition, as K decreases, the optimum angle becomes larger. Although we do not show it explicitly, it also turns

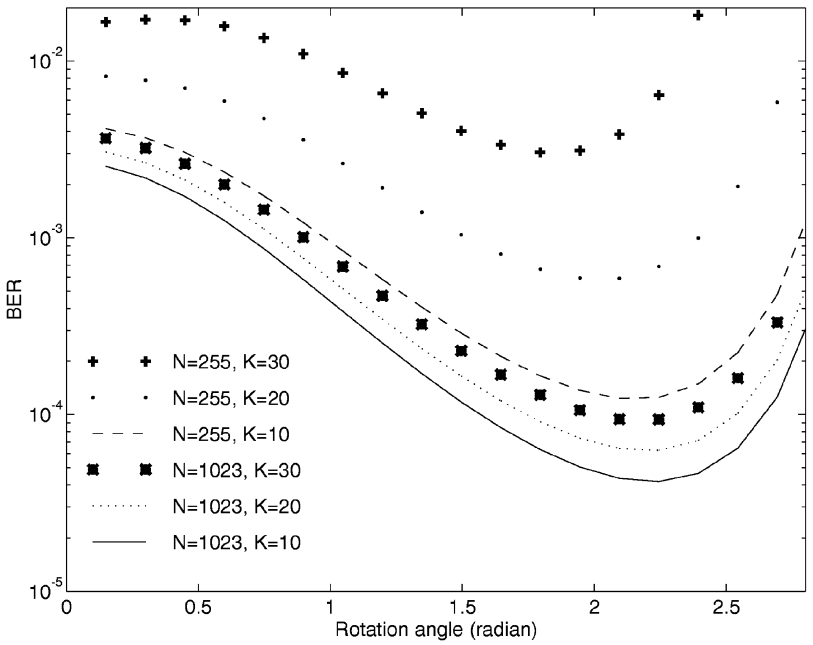

Fig. 4. The bit error probability versus the rotation angle when $L = 10$ and SNR $= 10$ dB.

out that, as L increases, the optimum value becomes larger.

Fig. 5 shows the optimum angle versus SNR for various system parameters. In this figure, we see that the optimum angle becomes large when N becomes long and K becomes small. Although we do not explicitly show, the optimum angle is expected to approach π as SNR $\to \infty$, since the free distance is maximized when $\phi = \pi$ [1]. In other words, if SNR $\to \infty$, there is no noise, and the free distance will be the most important factor to determine the system performance. Since the free distance of this system is $4 + 4\sin^2(\phi/2)$, the free distance has the maximum value when $\phi \to \pi$. In Fig. 6, the optimum angle versus the number K of users is shown as a function of L and N. When N is large, the optimum angle does not change much with K, which means that if we use a long spreading code, the optimum angle can be fixed even when the number of users may change to certain degree. We can also see that the optimum angle becomes large when L becomes large.

Some plots of the bit error probability versus SNR for the STCM and optimum ATCM schemes for various system parameters are shown in Fig. 7. The ATCM has better performance than the STCM as expected: depending on the system parameters, the ATCM scheme has $0.5 \sim 1.2$ dB gain approximately over the STCM. It is noteworthy to see from Fig. 7 that the ATCM scheme with $N = 127$ is expected to have better performance than the STCM scheme with $N = 511$ at SNR higher than 15 dB.

In Fig. 8, the bit error probability versus K is plotted: from this figure we see that the ATCM has a larger user capacity than the STCM. The difference in user capacity becomes more significant as N becomes larger. For instance, in Fig. 8, we can see that the difference between the user capacity of the ATCM and that of the STCM is approximately 10 when $N = 511$ and $P_b = 10^{-4}$.

In order to compare the results in Sections 3.1 and 3.2, some plots are shown in Fig. 9. When the SNR is low, the methods in Sections 3.1 and 3.2 produce similar upper bounds. As the SNR becomes higher, the difference between the two bounds becomes larger. In Fig. 9, we can see the

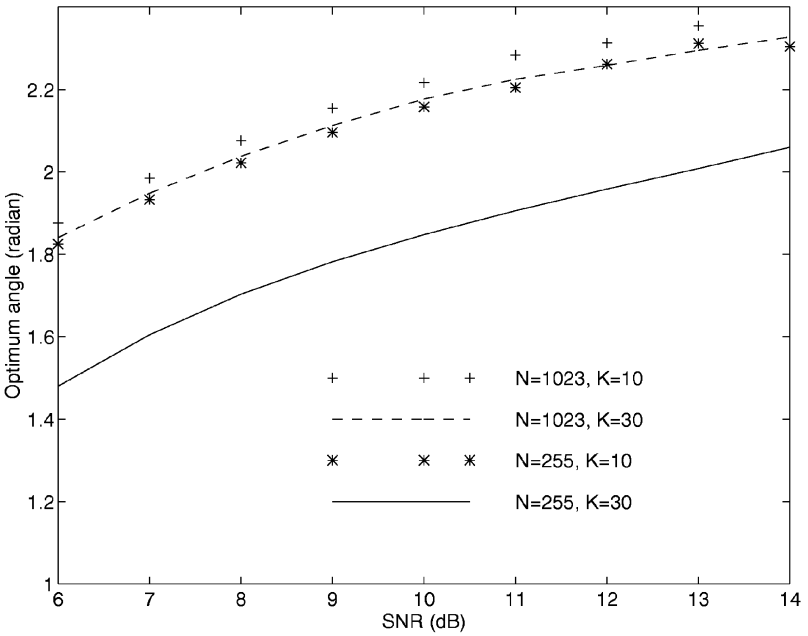

Fig. 5. The optimum angle versus SNR when $L = 10$.

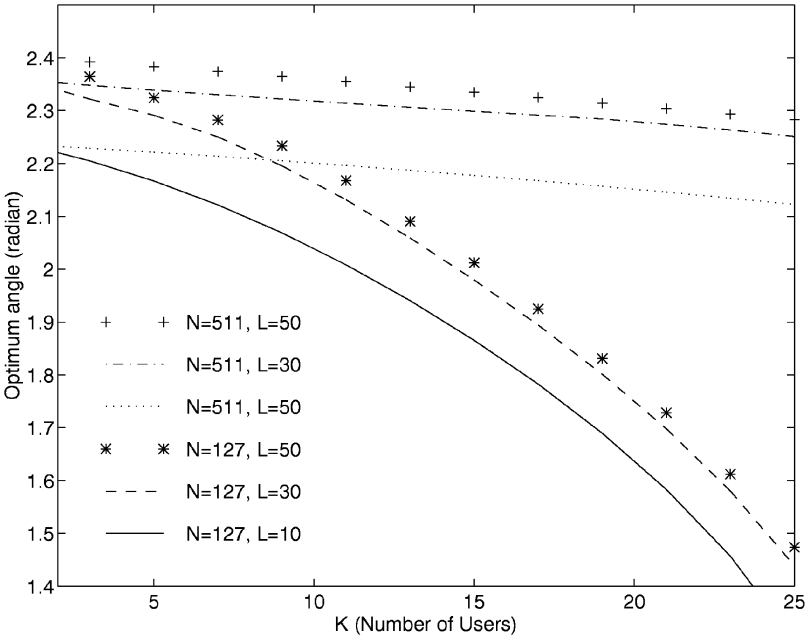

Fig. 6. The optimum angle versus the number of users when SNR = 10 dB.

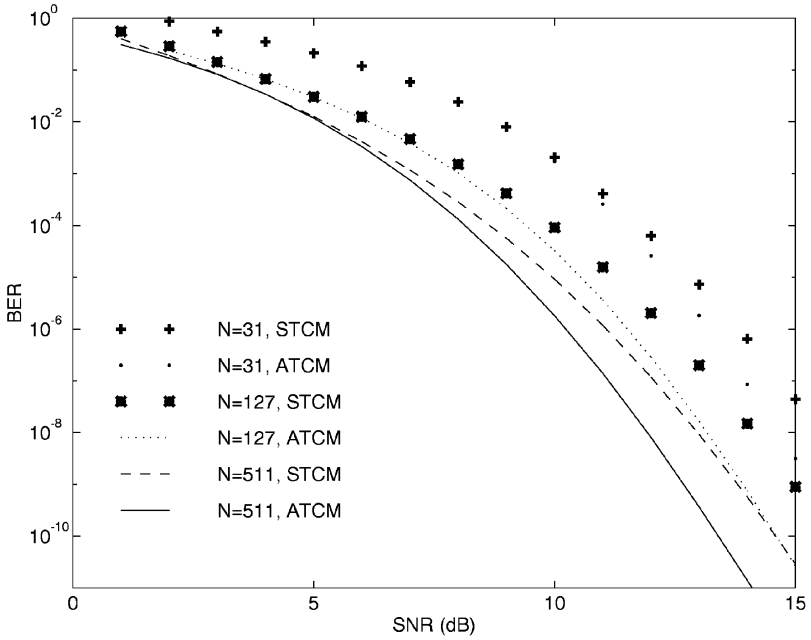

Fig. 7. The bit error probability versus SNR when $K = 10$ and $L = 10$ (STCM: symmetric TCM, ATCM: optimum asymmetric TCM).

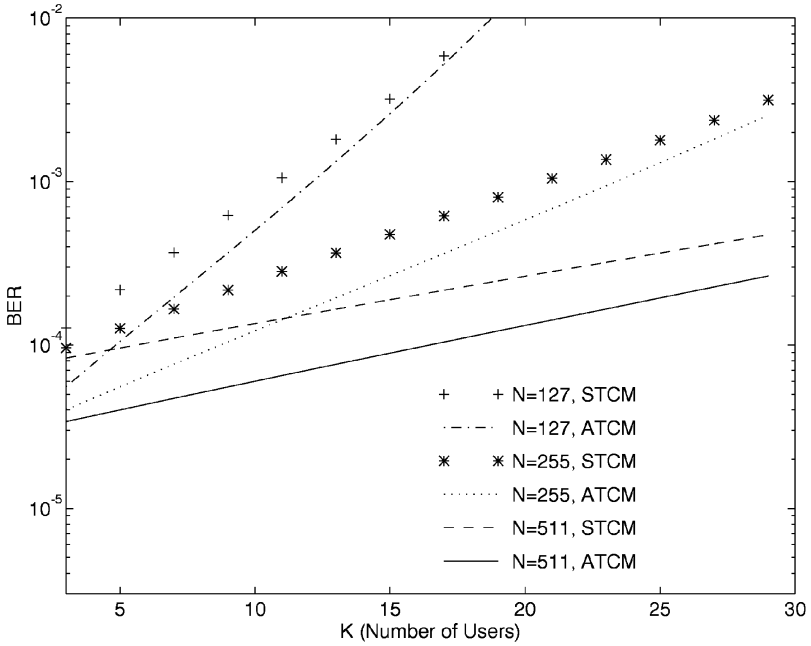

Fig. 8. The bit error probability versus the number of users when $L = 10$ and SNR $= 10$ dB (STCM: symmetric TCM, ATCM: optimum asymmetric TCM).

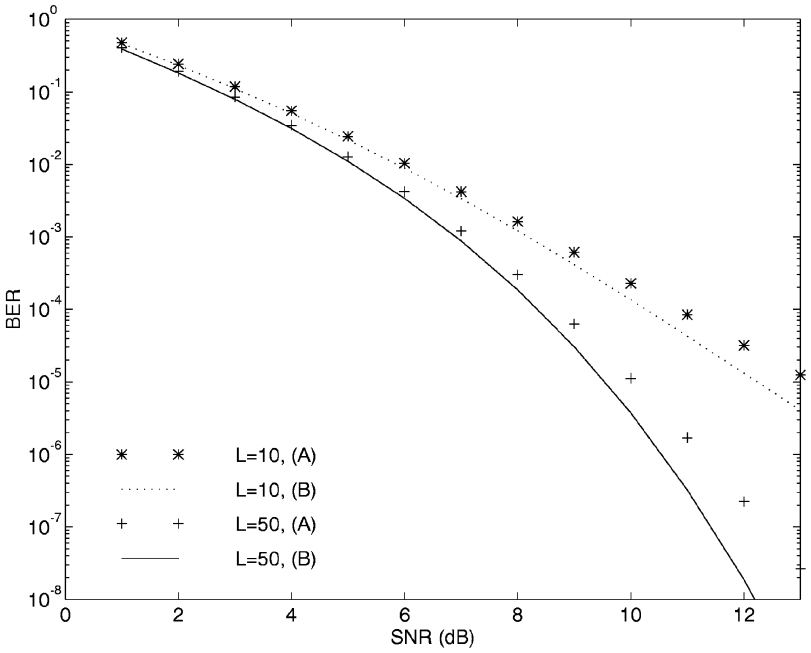

Fig. 9. The bit error probability versus SNR for Gaussian approximation and Taylor series expansion methods when $N = 127$ and $K = 10$. (A): bit error probability calculated from Eq. (36), (B): bit error probability calculated from Eq. (49).

Gaussian approximation of interuser interferences is overly optimistic as in [2].

In summary, the performance of the optimum ATCM scheme is better than that of the STCM: as the system environment becomes favorable (K becomes small, L becomes large, and N becomes long), the difference between the performance of the two schemes becomes bigger, and use of an optimum ATCM is therefore desirable, for example for very low bit error data communications. It is also shown that the optimum rotation angle does not change much with the number of users, when the value of the code length N is large. It should be mentioned that, since the code length is usually 1024 in practical CDMA systems, which can be considered long enough, we can expect $1 \sim 2$ dB gain with the ATCM scheme.

5. Concluding remark

In this paper, we obtained an upper bound of the DS/SSMA system performance using asymmetric TCM DS/SSMA signal constellation. For the 1/2 rate optimum asymmetric TCM schemes, we obtained the optimum rotation angles minimizing the upper bound of the bit error probability. The effects of the system parameters on the optimum angle and on the performance were also investigated.

Based on the results we may conclude that the optimum asymmetric TCM DS/SSMA scheme has better performance than the symmetric TCM DS/SSMA scheme. In addition, if the number of users is small, the SNR is high, and the fading is less severe, the optimum asymmetric TCM scheme is expected to have more SNR gain over the traditional symmetric scheme: this means that the optimum ATCM is useful in data communications, where very low bit error rate is required.

Acknowledgements

This research was supported by Korea Science and Engineering Foundation (KOSEF) under Grant 961-0923-134-2, for which the authors would like to express their thanks. The authors also wish to thank the anonymous reviewers for their constructive and helpful comments and suggestions.

Appendix A. Calculation of the fourth order term in Eq. (20)

The fourth-order term of the Taylor series is obtained as

$$\tfrac{1}{4}\lambda^4\rho_n^4|x_n - \hat{x}_n|^4 E|z_n|^4. \tag{A.1}$$

Let us first consider $E|z_n|^4$. From Eq. (8), z_n can be expressed as

$$z_n = \sum_{k=1}^{K-1} g_k, \tag{A.2}$$

where

$$g_k = \frac{1}{T}\{x_{n-1}^k R(\tau) + x_n^k \hat{R}(\tau)\}. \tag{A.3}$$

Then the fourth absolute moment of z_n is

$$\begin{aligned} E\left\{\left(\sum_{k=1}^{K-1} g_k\right)^2\left(\sum_{k=1}^{K-1} g_k^*\right)^2\right\} &= E\left\{\left(\sum_{k=1}^{K-1} g_k^2 + \sum_{i\neq j} g_i g_j\right)\left(\sum_{k=1}^{K-1} g_k^{*2} + \sum_{i\neq j} g_i g_j^*\right)\right\} \\ &= E\left\{\sum_{k=1}^{K-1} |g_k|^4\right\} + E\left\{\sum_{i\neq j} g_i^2 g_j^{*2}\right\} + 2E\left\{\sum_{i\neq j} |g_i|^2|g_j|^2\right\}. \end{aligned} \tag{A.4}$$

The first expectation on the right-hand side of Eq. (A.4) is

$$E\left\{\sum_{k=1}^{K-1}|g_k|^4\right\}=\sum_{k=1}^{K-1}E|g_k|^4, \tag{A.5}$$

where

$$\begin{aligned}E|g_k|^4 &= \frac{1}{T^4}E[|\{x_{n-1}^k R(\tau)+x_n^k\hat{R}(\tau)\}\{x_{n-1}^{k*}R(\tau)+x_n^{k*}\hat{R}(\tau)\}|^2]\\ &= \frac{1}{T^4}E[|x_{n-1}^k|^4R^4(\tau)+(x_{n-1}^k x_n^k)^2R^2(\tau)\hat{R}^2(\tau)+(x_n^k x_{n-1}^{k*})^2R^2(\tau)\hat{R}^2(\tau)+|x_n^k|^4\hat{R}^4(\tau)\\ &\quad +2\{|x_{n-1}^k|^2(x_{n-1}^k x_n^k)R^3(\tau)\hat{R}(\tau)+|x_{n-1}^k|^2(x_n^k x_{n-1}^{k*})R^3(\tau)\hat{R}(\tau)+|x_{n-1}^k|^2|x_n^k|^2R^2(\tau)\hat{R}^2(\tau)\\ &\quad +|x_{n-1}^k|^2x_n^{k^2}R^2(\tau)\hat{R}^2(\tau)+x_{n-1}x_n^k|x_n^k|^2R(\tau)\hat{R}^3(\tau)+x_n^k x_{n-1}^{k*}|x_n^k|^2R(\tau)\hat{R}(\tau)\}]\\ &= \frac{1}{T^4}[E\{R^4(\tau)\}+E\{\hat{R}^4(\tau)\}+2E\{R^2(\tau)\hat{R}^2(\tau)\}],\end{aligned} \tag{A.6}$$

since $E(x_n^k)=0$, $E(|x_n^k|^2)=1$, $E(x_n^{k^2})=0$ and $E(|x_n^k|^4)=1$ when $\Pr\{x_n^k=q\}=\frac{1}{4}$ for $q\in\{1,-1,i,-i\}$. In Eq. (A.6) we can show that

$$E\{R^4(\tau)\}+E\{\hat{R}^4(\tau)\}\cong\frac{2T^4}{5N} \tag{A.7}$$

and

$$E\{R^2(\tau)\hat{R}^2(\tau)\}\cong 0, \tag{A.8}$$

as in [7]. Then Eq. (A.5) becomes

$$E\left\{\sum_{k=1}^{K-1}|g_k|^4\right\}\cong\frac{2(K-1)}{5N}. \tag{A.9}$$

Now the second term on the right-hand side of Eq. (A.4) is, assuming that the interuser interference is uncorrelated,

$$\sum_{i\neq j}E(g_i^2g_j^{*2})=\sum_{i\neq j}E(g_i^2)E(g_j^{*2}). \tag{A.10}$$

It can be shown, as in Eq. (A.6), that

$$E(g_i^2)=E\{(x_{n-1}^iR(\tau))^2+(x_n^i\hat{R}(\tau))^2\}=0, \tag{A.11}$$

and thus Eq. (A.10) becomes

$$\sum_{i\neq j}E(g_i^2g_j^{*2})=0. \tag{A.12}$$

The third term on the right-hand side of Eq. (A.4) is obtained as [7]

$$2\sum_{i\neq j}E|g_i|^2E|g_j|^2\cong 8\frac{(K-1)(K-2)}{(3N)^2}, \tag{A.13}$$

which is quite small compared to Eq. (A.9) for typical values of $K \cong 20$ and $N = 511$. The fourth absolute moment of z_n is, using Eqs. (A.4), (A.9), (A.12) and (A.13),

$$E\left[\left|\frac{1}{T}\sum_{k=1}^{K-1} g_k\right|^4\right] \cong \frac{2(K-1)}{5N}. \tag{A.14}$$

Therefore, we have

$$\frac{\text{fourth-order term}}{\text{second-order term}} \cong \frac{1}{4}\lambda^2\rho_n^2|x_n - \hat{x}_n|^2\frac{1}{4} = \frac{3}{160\sigma_\eta^4}, \tag{A.15}$$

where σ_η^2 is the noise variance when the signal power is normalized to 1. Thus when the SNR is high, the Taylor series in Eq. (20) converges slowly. When the SNR is low, however, the Taylor series converges rapidly and the approximation (22) would result in a reasonable approximation to λ_0.

Appendix B. Approximation of the Chernoff parameter

Consider the conditional pairwise error probability (23),

$$P(\boldsymbol{x} \to \hat{\boldsymbol{x}}|\boldsymbol{\rho}) \leqslant \prod_{n\in v} \exp\{-\lambda\rho_n^2|x_n - \hat{x}_n|^2(1 - 2\lambda\sigma_\eta^2)\}(1 + \lambda^2\rho_n^2|x_n - \hat{x}_n|^2\sigma_z^2). \tag{B.1}$$

The optimum λ minimizing the upper bound in Eq. (B.1) cannot be obtained analytically, since it depends on the index set v. Thus, in practice, one can only evaluate the bound using some fixed value of λ, which will be optimum for only one particular path length. Even so, a tight bound can still be obtained [1].

Differentiating a term on the right-hand side of Eq. (B.1) would result in a polynomial of the third order with respect to λ,

$$a\lambda^3 + b\lambda^2 + c\lambda + d = 0, \tag{B.2}$$

where

$$a = 4\rho_n^4|x_n - \hat{x}_n|^4\sigma_n^2\sigma_z^2, \tag{B.3}$$

$$b = -\rho_n^4|x_n - \hat{x}_n|^4\sigma_z^2, \tag{B.4}$$

$$c = 2\rho_n^2|x_n - \hat{x}_n|^2(2\sigma_n^2 + \sigma_z^2) \tag{B.5}$$

and

$$d = -\rho_n^2|x_n - \hat{x}_n|^2. \tag{B.6}$$

The solution to Eq. (B.2) is

$$\lambda_s = -\frac{b}{3a} - \frac{2^{1/3}Q}{3a(R + \sqrt{4Q^3 + R^2})^{1/3}} + \frac{(R + \sqrt{4Q^3 + R^2})^{1/3}}{3\cdot 2^{1/3}a}, \tag{B.7}$$

where

$$Q = 48|x_n - \hat{x}_n|^6\rho_n^6\sigma_\eta^4\sigma_z^2 - |x_n - \hat{x}_n|^8\rho_n^8\sigma_z^4 + 24|x_n - \hat{x}_n|^6\rho_n^6\sigma_\eta^2\sigma_z^4 \tag{B.8}$$

and

$$R = 288|x_n - \hat{x}_n|^{10}\rho_n^{10}\sigma_\eta^4\sigma_z^4 + 2|x_n - \hat{x}_n|^{12}\rho_n^{12}\sigma_z^6 - 72|x_n - \hat{x}_n|^{10}\rho_n^{10}\sigma_\eta^2\sigma_z^6. \tag{B.9}$$

When $\sigma_z^2 \gg \sigma_n^2$, Q and R can be approximated as

$$Q = -|x_n - \hat{x}_n|^8 \rho_n^8 \sigma_z^4 \left\{1 - \frac{24\sigma_\eta^2}{|x_n - \hat{x}_n|^2 \rho_n^2}\left(1 + \frac{2\sigma_\eta^2}{\sigma_z^2}\right)\right\} \cong -|x_n - \hat{x}_n|^8 \rho_n^8 \sigma_z^4 \tag{B.10}$$

and

$$R = 2|x_n - \hat{x}_n|^{12} \rho_n^{12} \sigma_z^6 \left\{1 - \frac{36\sigma_\eta^2}{|x_n - \hat{x}_n| \rho_n^2}\left(1 - \frac{4\sigma_\eta^2}{\sigma_z^2}\right)\right\} \cong 2|x_n - \hat{x}_n|^{12} \rho_n^{12} \sigma_z^6, \tag{B.11}$$

from which

$$(R + \sqrt{4Q^3 + R^2})^{1/3} \cong R^{1/3}, \tag{B.12}$$

since $4Q^3 + R^2 \cong 0$.

Using Eqs. (B.3), (B.4), (B.10) and (B.12) in Eq. (B.7), λ_s is obtained approximately as

$$\lambda_s \cong -\frac{1}{12\sigma_n^2} - \frac{2^{1/3} Q}{3aR^{1/3}} + \frac{R^{1/3}}{3 \cdot 2^{1/3} a} = \frac{1}{4\sigma_\eta^2}. \tag{B.13}$$

The value of λ_s in Eq. (B.13) is the same as that when there exists Gaussian noise only in the system. In addition, if we assume the multiuser interference is Gaussian and let $\sigma_n^2 \to \sigma_n^2 + \sigma_z^2$, then it is the same as λ_G obtained in Section 3.2. Since $\sigma_z^2 = 2(K-1)/3N \cong 0.03$ typically, the condition $\sigma_z^2 \gg \sigma_n^2$ implies high SNR. Therefore, Eq. (B.13) is a good approximation to Eq. (B.7) for high SNR.

References

[1] E. Biglieri, D. Divsalar, P.J. Mclane, M.K. Simon, Introduction to Trellis Coded Modulation with Applications, Macmillan, New York, 1991.

[2] G.D. Boudreau, D.D. Falconer, S.A. Mahmoud, A comparison of trellis coded versus convolutionally coded spread spectrum multiple access systems, IEEE J. Selec. Areas Commun. JSAC-8 (May 1990) 628–640.

[3] D. Divsalar, M.K. Simon, J.H. Yuen, Trellis coding with asymmetric modulations, IEEE Trans. Commun. COM-35 (February 1987) 130–141.

[4] E.A. Geraniotis, Direct sequence spread spectrum multiple access communication over nonselective and frequency selective Rician fading channels, IEEE Trans. Commun. COM-34 (August 1986) 756–764.

[5] J.S. Lee, R.H. French, L.E. Miller, Probability of error analyses of a BFSK frequency-hopping systems with diversity under partial band jamming interference – Part I: Performance of square-law linear combining soft decision receiver, IEEE Trans. Commun. COM-32 (June 1984) 645–653.

[6] M.B. Pursley, Performance evaluation for phase coded spread spectrum multiple access communication Part I: System analysis, IEEE Trans. Commun. COM-25 (August 1977) 795–799.

[7] M.B. Pursley, Performance evaluation for phase-coded spread spectrum multiple access communication – Part II: Code sequence analysis, IEEE Trans. Commun. COM-25 (August 1977) 800–803.

[8] G. Ungerboeck, Channel coding with multilevel/phase signals, IEEE Trans. Inform. Theory IT-28 (1982) 55–67.

[9] B.D. Woerner, W.E. Stark, Trellis-coded direct-sequence spread-spectrum communications, IEEE Trans. Commun. COM-42 (December 1994) 3161–3170.